Electronic Supplementary Material (ESI) for CrystEngComm.
This journal is © The Royal Society of Chemistry 2023

Dual control of passive light output direction by light and mechanical forces in elastic crystals

Chuchu Han,[a] Jing Yang,[a] Xin Zhang,[c] Aisen Li,*[b] Jiang Peng*[a]

[a] Key Laboratory of Magnetic Molecules and Magnetic Information Materials of Ministry of Education & School of Chemistry and Materials Science of Shanxi Normal University, Taiyuan, 030032, PR China

E-mail address: 464831869@qq.com (J. P.).

[b] School of Physical Science and Information Technology, Shandong Key Laboratory of Optical Communication Science and Technology, Liaocheng University, Liaocheng, 252059, China. Email: liaisen@lcu.edu.cn (A. S. L.)

[c] Aerospace science & industry defense technology research and test center, Beijing, 100039, China.

Experimental methods

^{1}H NMR (600 MHz) and ^{13}C NMR (151 MHz) spectra were performed using a Mercury Plus instrument. The samples for irradiation time-dependent ^{1}H NMR measurements were obtained via the irradiation of the micro-crystals of **BPMP** by 365 nm (3 W) light for different times, followed by dissolving in DMSO-d_6. The samples for heating time-dependent ^{1}H NMR measurements were gained via the irradiation of the microcrystals of **BPMP** by 365 nm (3 W) light for 10 min, then, heating the microcrystals for 1 h and 4 h at 120 ℃, followed by dissolving in DMSO-d_6. HR-MS were recorded with Bruker Impact II in MeOH. Under nitrogen conditions, DSC and TGA were tested on Q200F3 instrument at a heating rate of 10 ℃·min^{-1}.

The UV-vis absorption and fluorescence emission spectra were obtained from VARIAN Cary 5000 and Cary Eclipse spectrophotometers, respectively.

Single crystal of **BPMP** was tested on the Rigaku RA XIS-RA PID diffractometer (CuKα, λ = 1.54178 Å). The test process was maintained at 150.00 K, The needle-like crystal of **BPMP** was obtained in Dichloromethane/MeOH (v/v = 2/8 mL).

The UV-103C UV flashlight was purchased commercially, 365 nm, 3 W, 58258 μ W/cm^2@15 cm.

Investigation of the photomechanical behavior: 1) Affix the crystal to a glass tube by means of adhesive, ensuring that it is suspended in the middle. 2) Illuminate the crystal with ultraviolet light at a temperature of 293 K and capture its motion using a video camera (**Figure S4a**).

Investigation of the heating recovery behavior: In order to better heat the crystals, we selected suitable crystals and placed them on a clean quartz sheet, and then placed the quartz sheet along with the crystals on a heating plate at a temperature of 373 K. A video camera was utilized to record the movement of the crystals.

Spatial optical and mechanical force control of passive light output direction: Firstly, the needle-like crystal was bonded to the optical fiber and fixed. Secondly, we placed another optical fiber at the end of the laser pointer to transmit the light (635 nm, 5 mW), and then

moved the laser pointer so that the end of the optical fiber was in contact with the crystal. Lastly, the passive light transmission process of the crystal was recorded under a microscope by irradiating the crystal with UV light (365 nm, 3 W) and bending the crystal by force (**Figure S4b**).

Hirshfeld surfaces and 2 D fingerprint plots of **BPMP** were calculated using Crystal explorer 17.

The reaction cavity volumes of **BPMP** were calculated using cavity (SV) program.

The **BPMP** morphology of the crystal was simulated using the CSD-particle feature of mercury software based on the CIF file (CCDC deposit 2285149).

Frontier molecular orbitals, energy band gaps, and TD-DFT calculations of **BPMP** were performed by the Gaussian 09W program.

Frequency factor, activation energy and half-life calculations: 1) ***E*-BPMP** was prepared as a 10^{-5} M solution in DMF. 2) The solution was irradiated with UV light and the corresponding absorption spectra were tested (***E*-BPMP** was gradually converted to ***Z*-BPMP**) until the absorption intensity stopped changing. 3) The absorption spectra of the solution were tested over time at 298 K. 4) The above test was repeated with the only difference being that at 343 K , the absorption spectra of the compounds were tested over time. 5) Calculate the frequency factor, activation energy and half-life of the compounds based on the previous literature.[1, 2]

Synthesis and characterizations

(*E*)-N'-([1,1'-biphenyl]-4-ylmethylene)picolinohydrazide (**BPMP**)

[1,1'-biphenyl]-4-carbaldehyde (1.00 g, 3.64 mmol) and picolinohydrazide (0.753 g, 3.64 mmol)were stirred at 80 ℃ for 6 h in ethanol (50 mL). Then the mixture was cooled to room temperature and filtered off. The precipitates recrystallized in ethanol to obtain white solid (0.856 g, 78%). M.p.: 218-220 ℃. ^{1}H NMR (600 MHz, DMSO-d_6) δ 12.20 (s, 1H), 8.735 (d, J = 6.0 Hz, 1H), 8.71 (s, 1H), 8.155 (d, J = 6.0Hz, 1H), 8.08 (t, J = 6.0 Hz, 1H), 7.815 (q, J = 6.0 Hz，2H), 7.745 (d, J = 6.0 Hz, 1H), 7.69 (t, J = 6.0 Hz, 1H), 7.50 (t, J = 12.0 Hz, 2H), 7.41 (t, J = 6.0 Hz, 1H) (Figure S18). ^{13}C NMR (151 MHz, $CDCl_3$) δ 160.06, 149.19, 148.48, 148.09, 143.28, 140.27, 137.68, 132.62, 128.90, 128.35, 127.82, 127.37, 127.11, 126.78,

122.97 (Figure S19). HR-MS (ESI): m/z calcd for $C_{19}H_{15}N_3O$ $[M+Na]^+$: 324.1107, found: 324.1117 (Figure S20).

Table S1. Photophysical data of **BPMP** .

Compound	**Absorption[a] (nm)** **(ε/×10^5 M^{-1}cm^{-1})**		**Emission[b] (nm)**	
	acetonitrile	crystal	acetonitrile	crystal
BPDT	267 (0.13) 322 (0.42)	296 378	412	435

[a] Maximal absorption peak in acetonitrile (1.0×10^{-5} M) and crystal.

[b] Maximal emission peak in acetonitrile (1.0×10^{-5} M) and crystal.

Table S2. Main electronic transitions calculated with **TD-DFT**.

λ_{abc}[a] (nm)	**f[b]**	**Transition (%)[c]**
348.96	1.1744	H→L (98.7)
291.82	0.3223	H→L+1 (96.3)

[a]Computed absorption in acetonitrile; [b]Compound oscillator strength; [c]H represent HOMO, L represent LUMO.

Table S3. Computed vertical excitation spectra of **BPMP** in acetonitrile at ground state.

Excited State	**Transition**	**Bandgap (eV)**	**Absorption (nm)**	**Oscillator strength**
Singlet (S_1)	H-L (98.7%)	3.5530	348.96	1.1744
Singlet (S_2)	H-4-L (87.9%) H-4-L+1 (8.8%)	4.1336	299.94	0.0007
Singlet (S_3)	H-L+1 (96.6%)	4.2487	291.82	0.3223

Table S4. The rate constants ($k_{\triangle}$), frequency factor (A), activation energy (E_a) and half-life ($\tau_{1/2}$) for the thermal *Z*→*E* isomerization process of **BPMP** in the dark in DMF solution.

Temperature (K)	$k_{\triangle}$ (s^{-1})	A (s^{-1})	E_a (kJ/mol)	$\tau_{1/2}$ (min)
298	3.30×10^{-4}	1.626	40.85	35.01
343	2.87×10^{-3}	1.505		4.03

Table S5. The hardness (*H*) and elasticity modulus (*E*) in the single crystal (002) face of **BPMP**.

Mechanical properties	1	2	3	4	Average value
H, GPa	0.04956	0.04673	0.04285	0.04036	0.045±0.007
E, GPa	0.25179	0.21927	0.19711	0.17763	0.211±0.055

Table S6. Single crystal data of **BPMP**.

	BPMP
Formula	$C_{19}H_{15}N_3O$
Formula weight	301.34
Temperature/K	150.00(10)
Space group	Pbca
Crystal system	orthorhombic
a (Å)	12.4347(5)
b (Å)	7.2040(3)
c (Å)	33.7027(13)
α (deg)	90
β (deg)	90
γ (deg)	90
V ($Å^3$)	3019.1(2)
Z	8
Dcalc(g/cm^3)	1.326
μ (mm^{-1})	0.673
F(000)	1264.0
Radiation	CuKα (λ = 1.54178)
2Θ range for data collection/°	5.244 to 147.07
Index ranges	$-6 \le h \le 15$, $-8 \le k \le 8$, $-39 \le l \le 41$
Reflections collected	7579
Independent reflections	2983 [R_{int} = 0.0477, R_{sigma} = 0.0528]
Data/restraints/parameters	2983/0/208
Final R indexes [I>=2σ (I)]	R_1 = 0.0539, wR_2 = 0.1338
Final R indexes [all data]	R_1 = 0.0690, wR_2 = 0.1490
Largest diff. peak/hole / e $Å^{-3}$	0.21/-0.27
Goodness-of-fit on F^2	1.036
CCDC	2285149

Table S7. Stabilization energies (in kJ/mol) of the individual molecular pairs associated with different intermolecular interactions

Number	Symmetry operation	R[a], Å	Electron Density	E_{ele}	E_{pol}	E_{dis}	E_{rep}	E_{tot}[b]
1	-x+1/2, y+1/2, z	3.62	B3LYP/6-31G(d,p)	-38.0	-9.5	-80.0	76.5	-69.5
2	-x, y+1/2, -z+1/2	10.03	B3LYP/6-31G(d,p)	0.1	-0.2	-1.3	0.0	-1.1
3	x+1/2, y, -z+1/2	9.09	B3LYP/6-31G(d,p)	-7.9	-4.1	-24.8	18.8	-21.4
4	x+1/2, -y+1/2, -z	11.97	B3LYP/6-31G(d,p)	-2.3	-1.3	-12.1	6.8	-9.8
5	x, -y+1/2, z+1/2	16.86	B3LYP/6-31G(d,p)	0.1	-0.4	-8.3	4.0	-5.0
6	-x, -y, -z	12.58	B3LYP/6-31G(d,p)	-17.8	-6.1	-14.4	11.6	-28.6

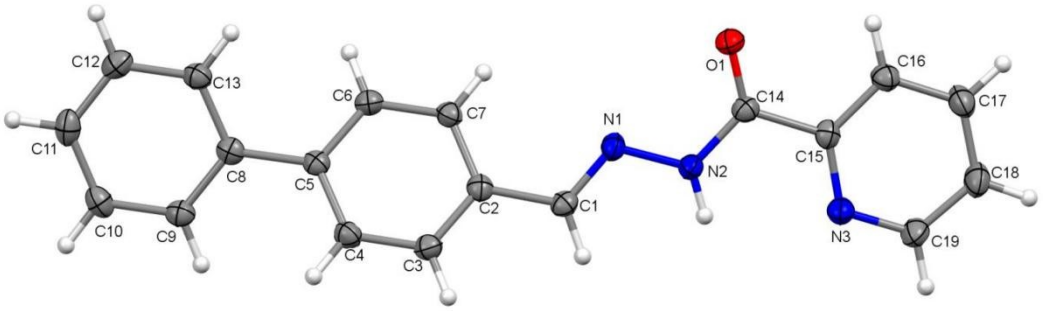

Figure S1. *ORTEP*of **BPMP** drawn with 50% ellipsoidal probability.

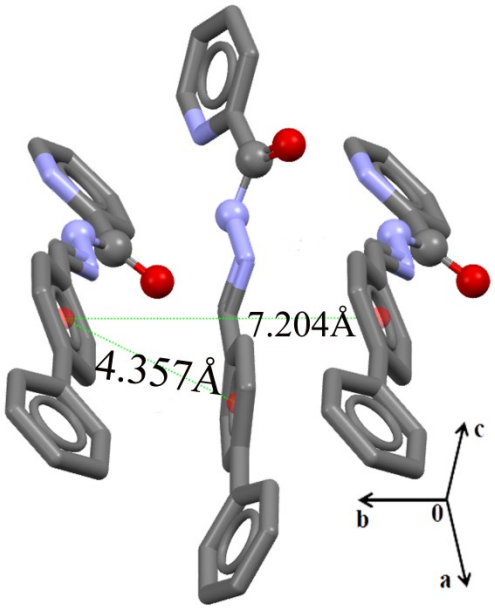

Figure S2. π···π interaction of **BPMP** molecules in crystal.

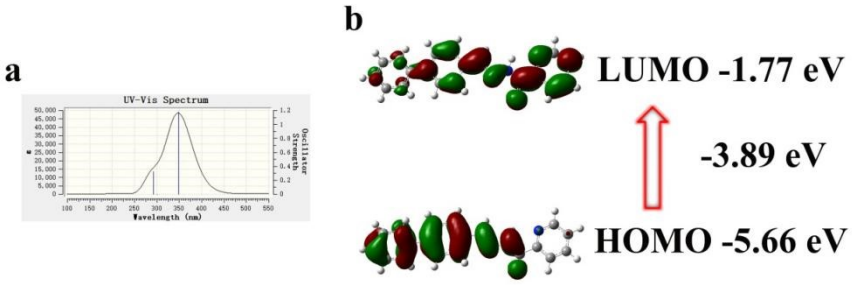

Figure S3. The calculated UV-Vis spectra of **BPMP** molecules obtained by TD-DFT calculations at the Gaussian 09W program with the B3LYP/6-311G (d,p) basis set.

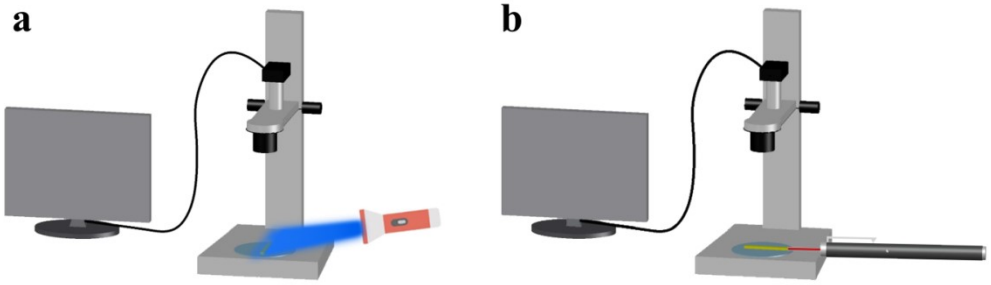

Figure S4. Schematic diagram of crystal mechanical bending (a) and passive waveguide testing (b).

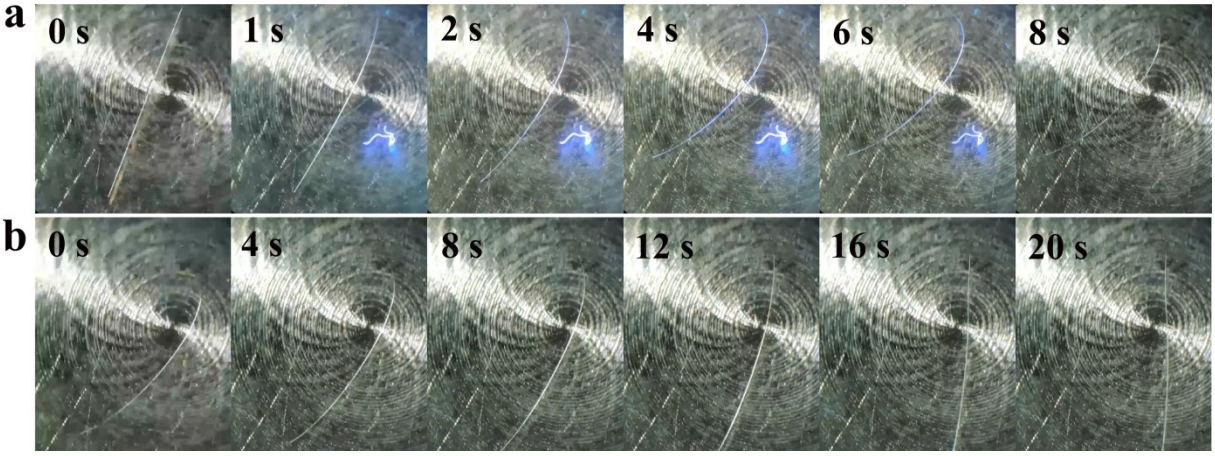

Figure S5. The photo-bending (Video S2) behavior of the needle-like crystal (8119 × 110 × 93 μm^3) of **BPMP** (a) and unbending (Video S3) by heating to 120 ℃ (b) (the photo time coincides with the video time).

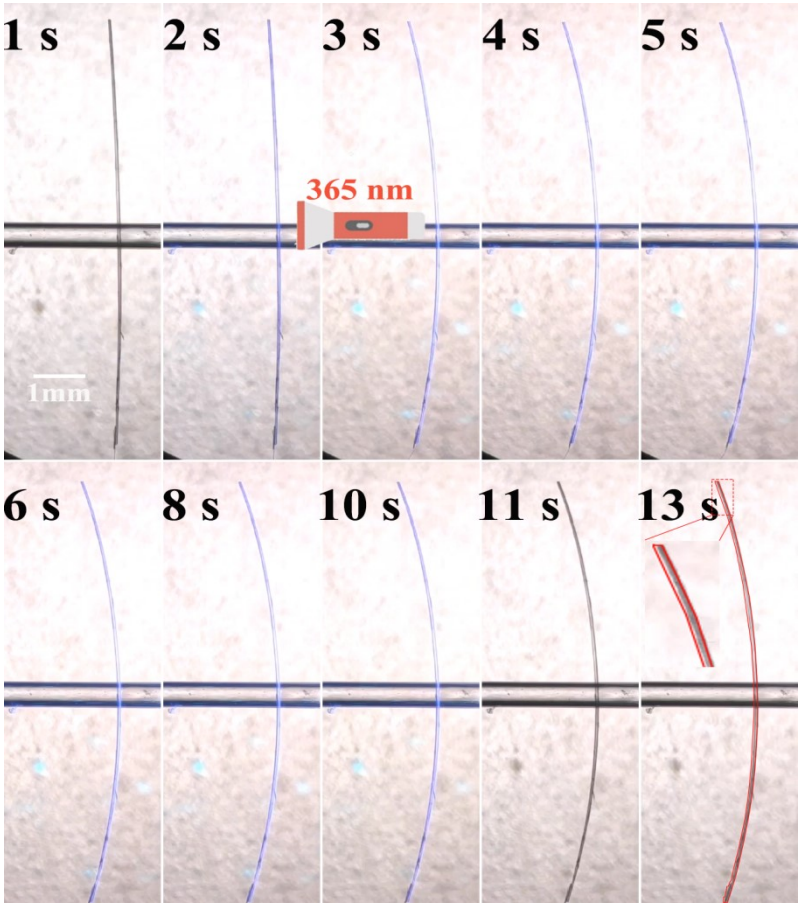

Figure S6. Photographic images of the **BPMP** crystal 1 (9479.42×106.37×82.93 μm^3, Video S5) driven by UV light (365 nm, 3W, 58258 μW/cm^2@15 cm). The red line shows the position of the crystal **BPMP** at 11 s (the photo time coincides with the video time, all images have the same scale bar).

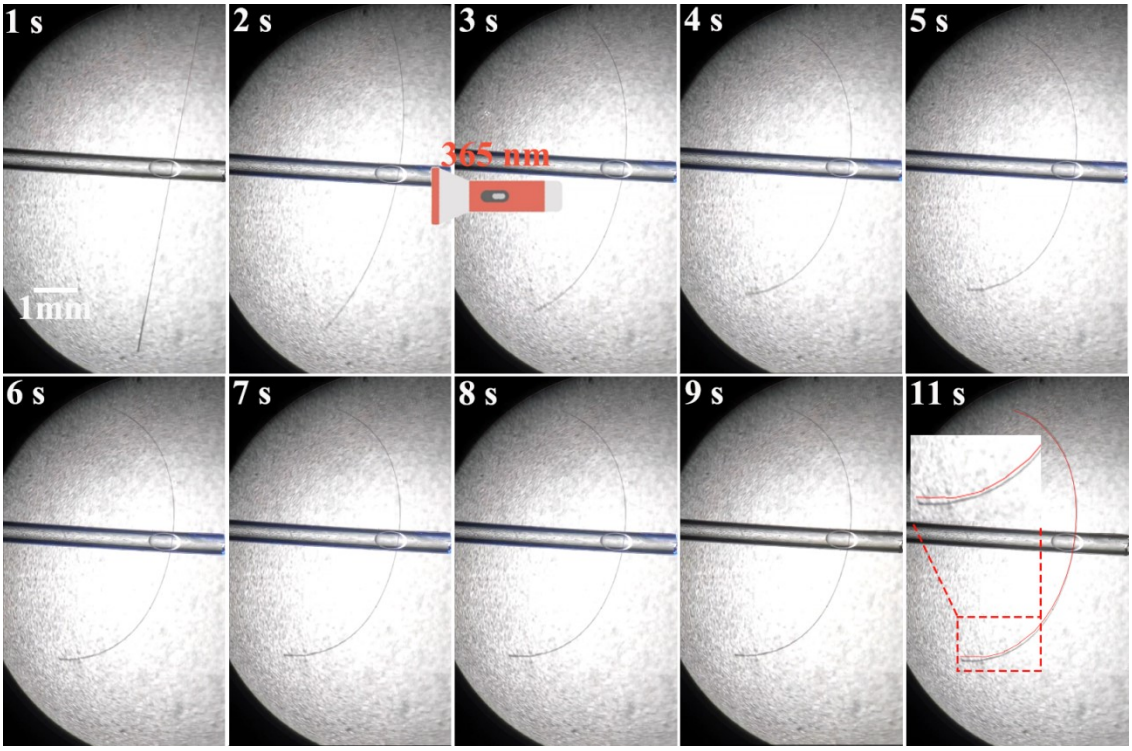

Figure S7. Photographic images of the **BPMP** crystal 3 (8003.09×39.52×34.78 μm^3, Video S6) driven by UV light (365 nm, 3W, 58258 μW/cm^2@15 cm). The red line shows the position of the crystal **BPMP** at 9 s (the photo time coincides with the video time, all images have the same scale bar .

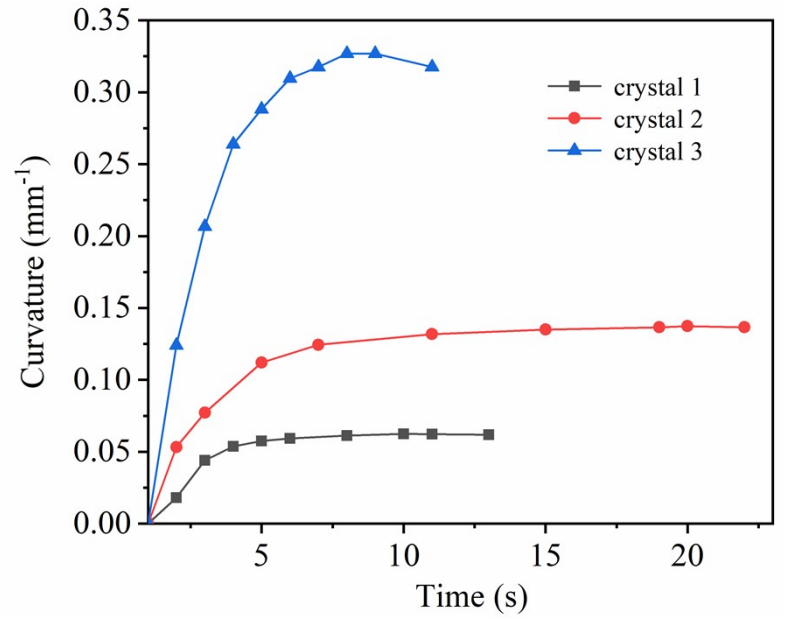

Figure S8. Curvature of the **BPMP** crystals of different sizes (black line, crystal 1, Video S1; red line, crystal 2, Video S5; blue line, crystal 3, Video S6) under UV irradiation.

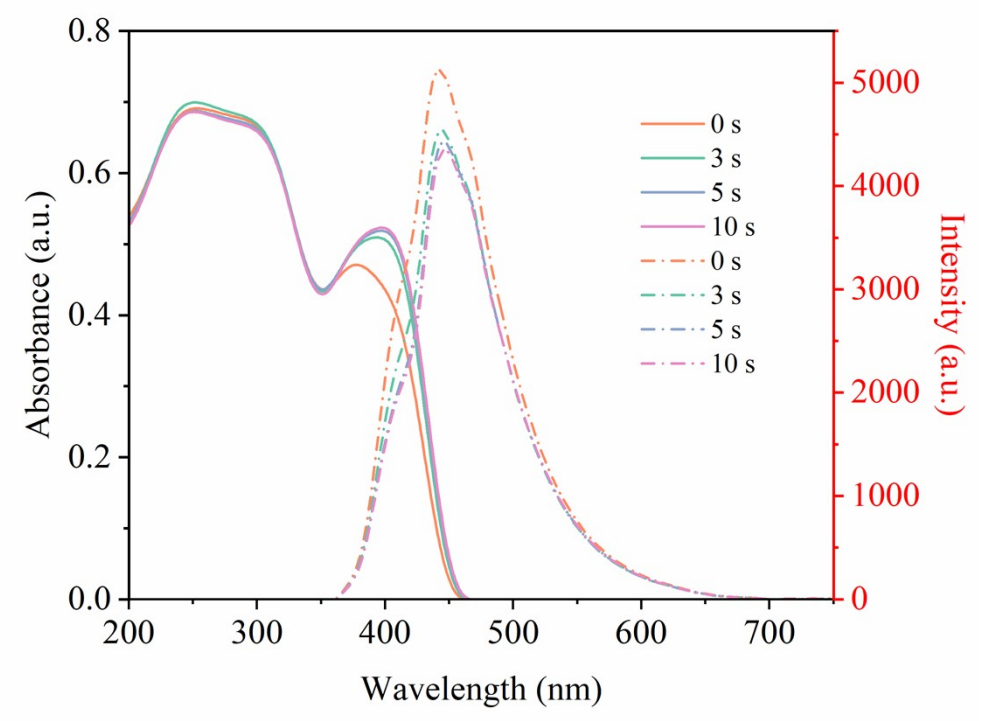

Figure S9. Time-dependent UV-vis absorption (solid line) and fluorescence emission (dot line, λ_{ex} = 320 nm) spectra of **BPMP** in microcrystals before and after irradiated by 365 nm (3 W) light sources for different times.

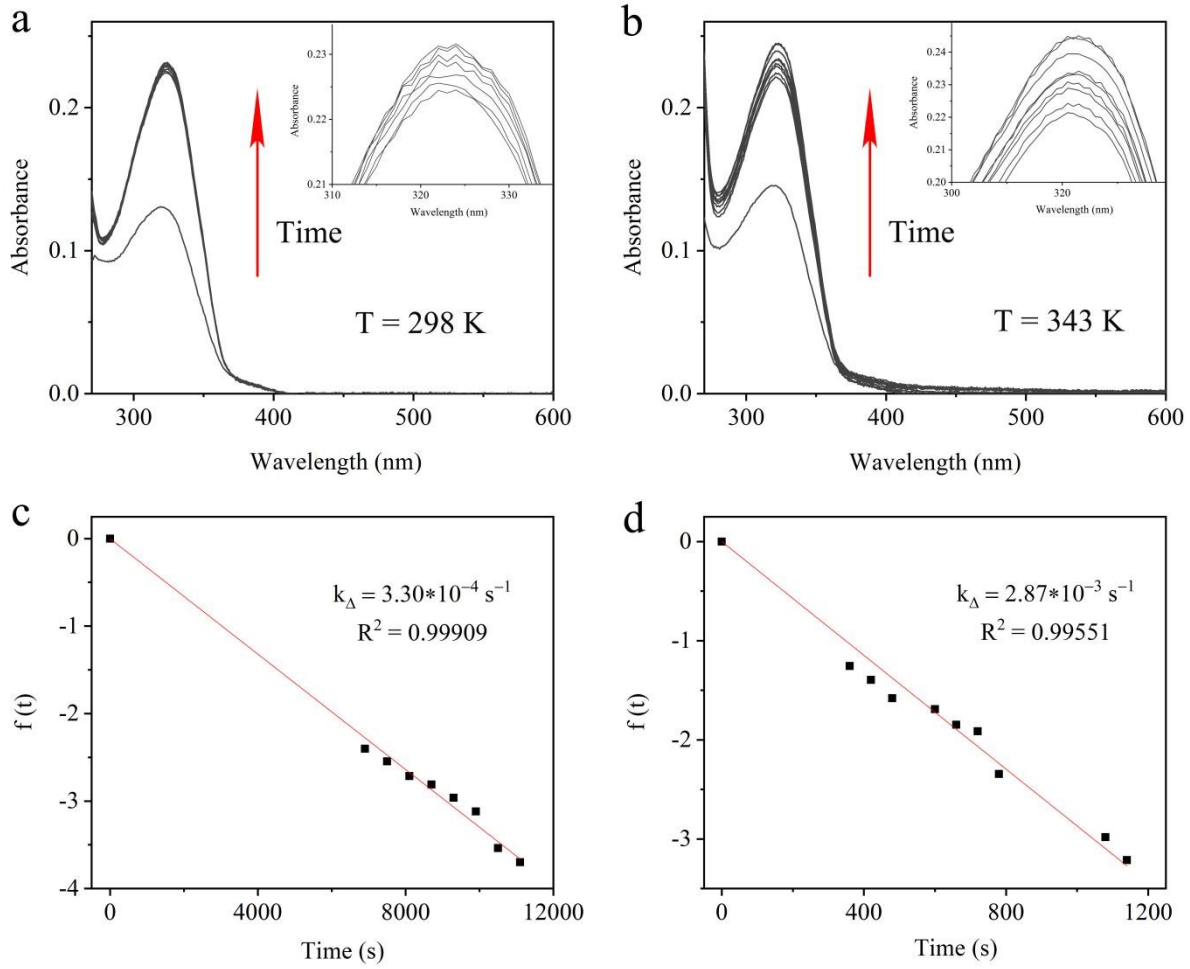

Figure S10. Changes in the absorbance due to the thermally driven *Z*→*E* isomerization of the **BPMP** in DMF solution measured at different temperatures: (a) 298 K and (b) 343 K; The plots allowing the determination of the rate constants $k_\triangle$ of the thermal *Z*→*E* isomerization reaction of **BPMP** at different temperatures (c, 298 K, d, 343 K), the absorbance change at λ= 323 nm was monitored.

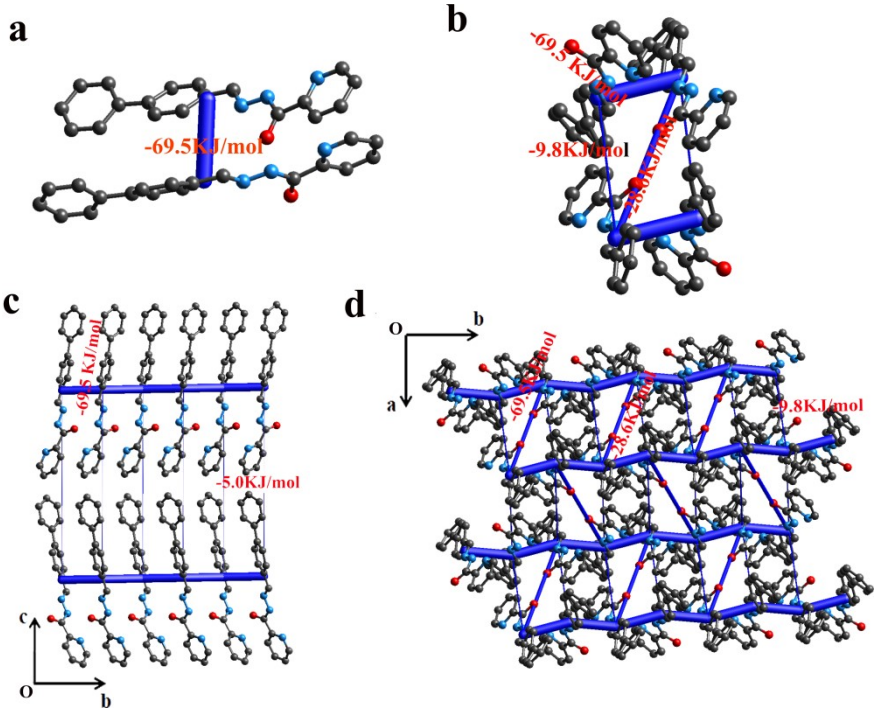

Figure S11. The total interaction energy of the **BPMP** crystal viewed down the a-axis (a, c) and c-axis (b, d).

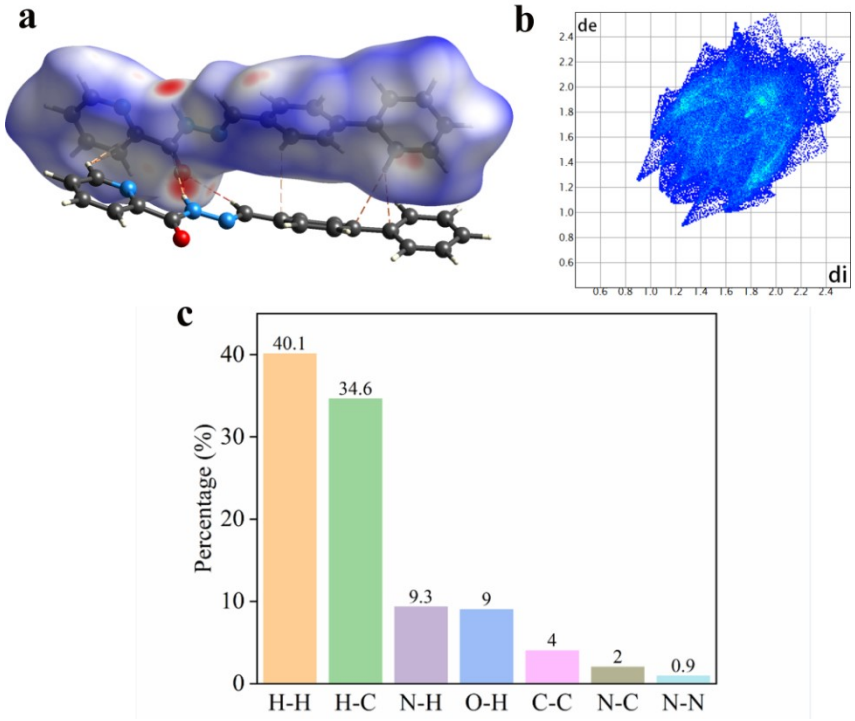

Figure S12. Hirshfeld surfaces mapped over d_{norm} of **BPMP** (a) with d_e (left) and d_i (right) mapped in colour (in both cases red represents the closest contacts, and blue the most distant contacts); 2 D fingerprint plots produced from the two functions for **BPMP** (b); The percentage of individual atomic contact contributions to the Hirshfeld surface for **BPMP** (c).

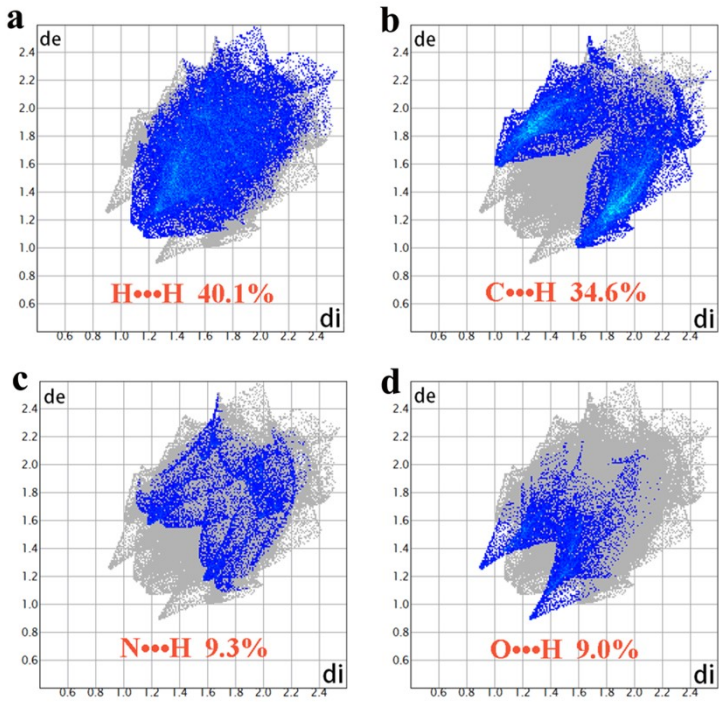

Figure S13. 2 D fingerprint plots produced from the H-H (a), C-H (b), N-H (c) and O-H (d) intermolecular interactions of **BPMP**.

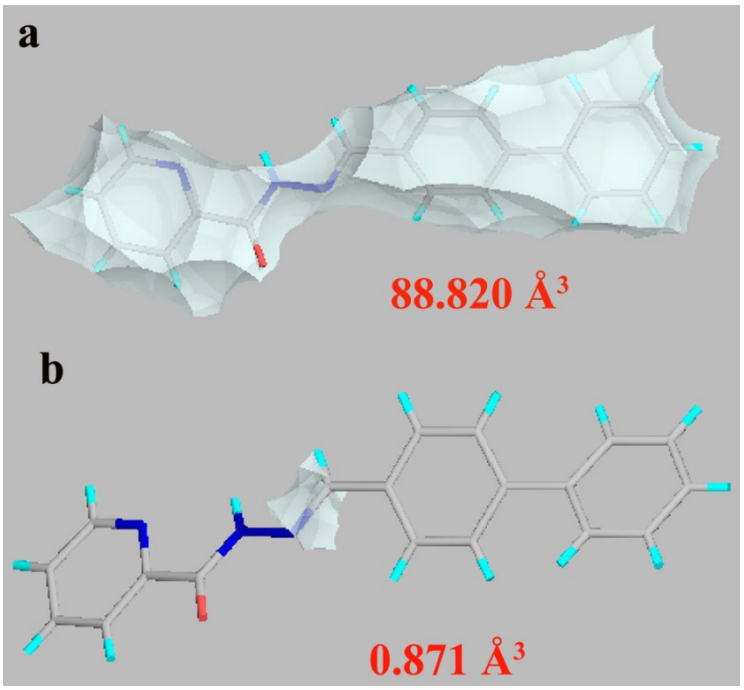

Figure S14. The reaction cavity of the **BPMP** molecule (a) and reaction cavity for the -C=N- moiety of **BPMP** (b).

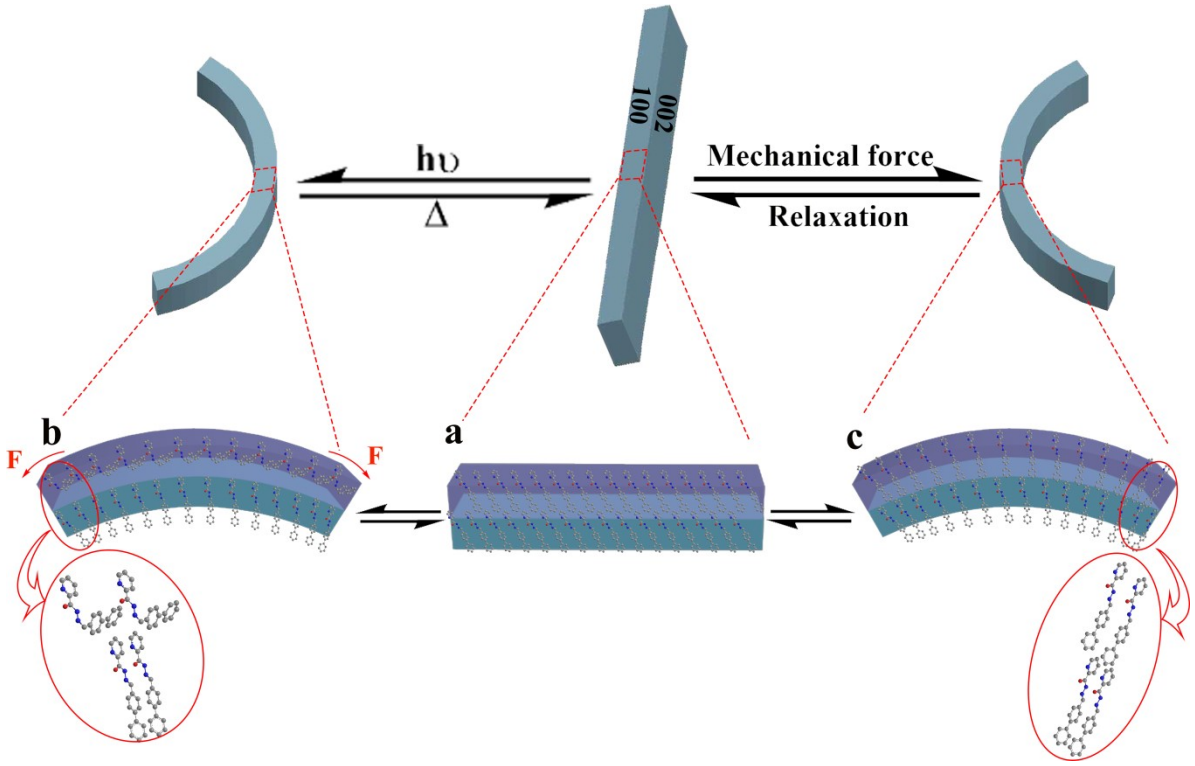

Figure S15. Schematic of light-induced (a→b) and mechanical force-induced bending (a→c) of **BPMP** crystal.

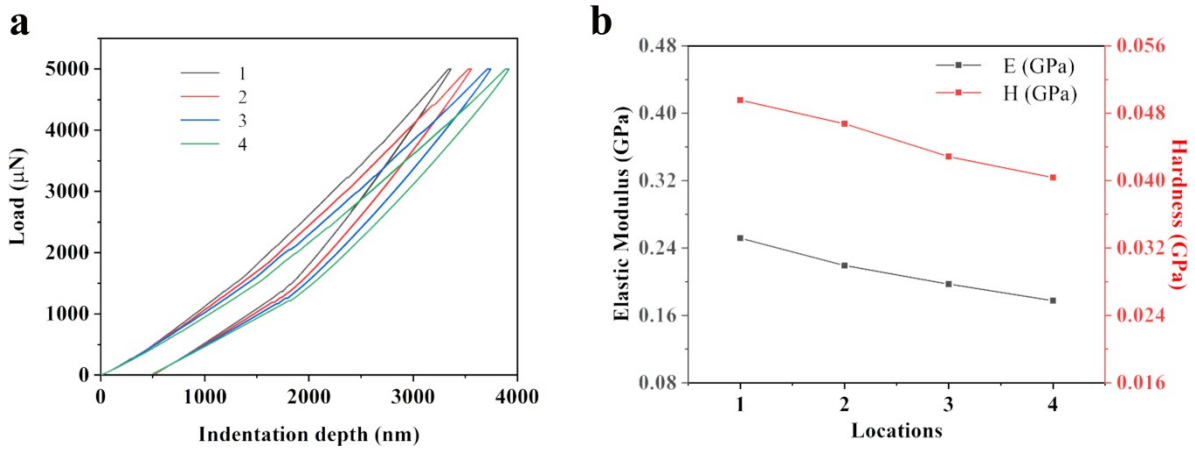

Figure S16. Load-depth curves of the **BPMP** crystal (a) ; elastic modulus (E) and hardness (H) of the (002) surface of the **BPMP** crystal (b).

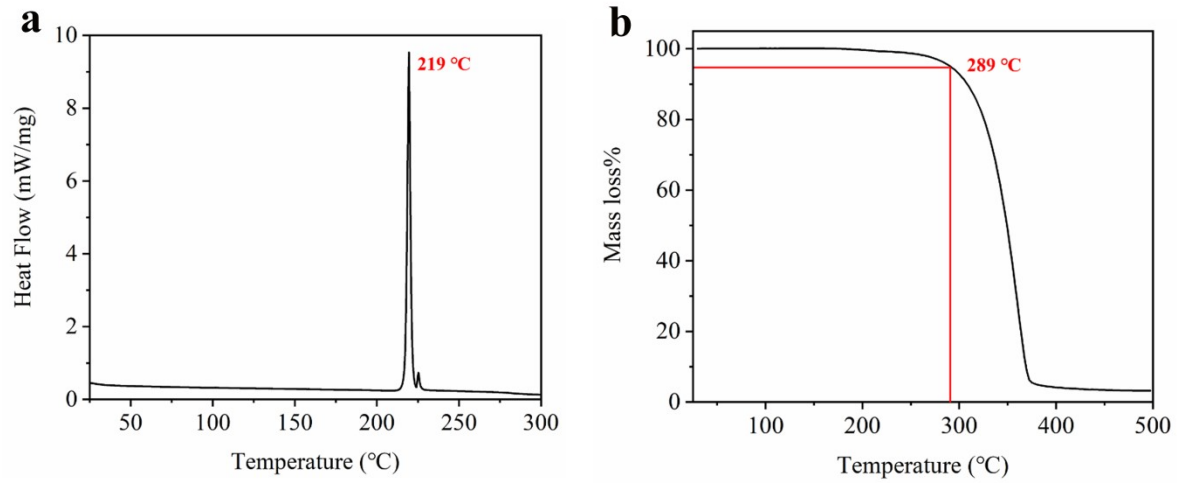

Figure S17. The differential scanning calorimetry (a) and thermogravimetric analysis (b) traces of **BPMP** crystal.

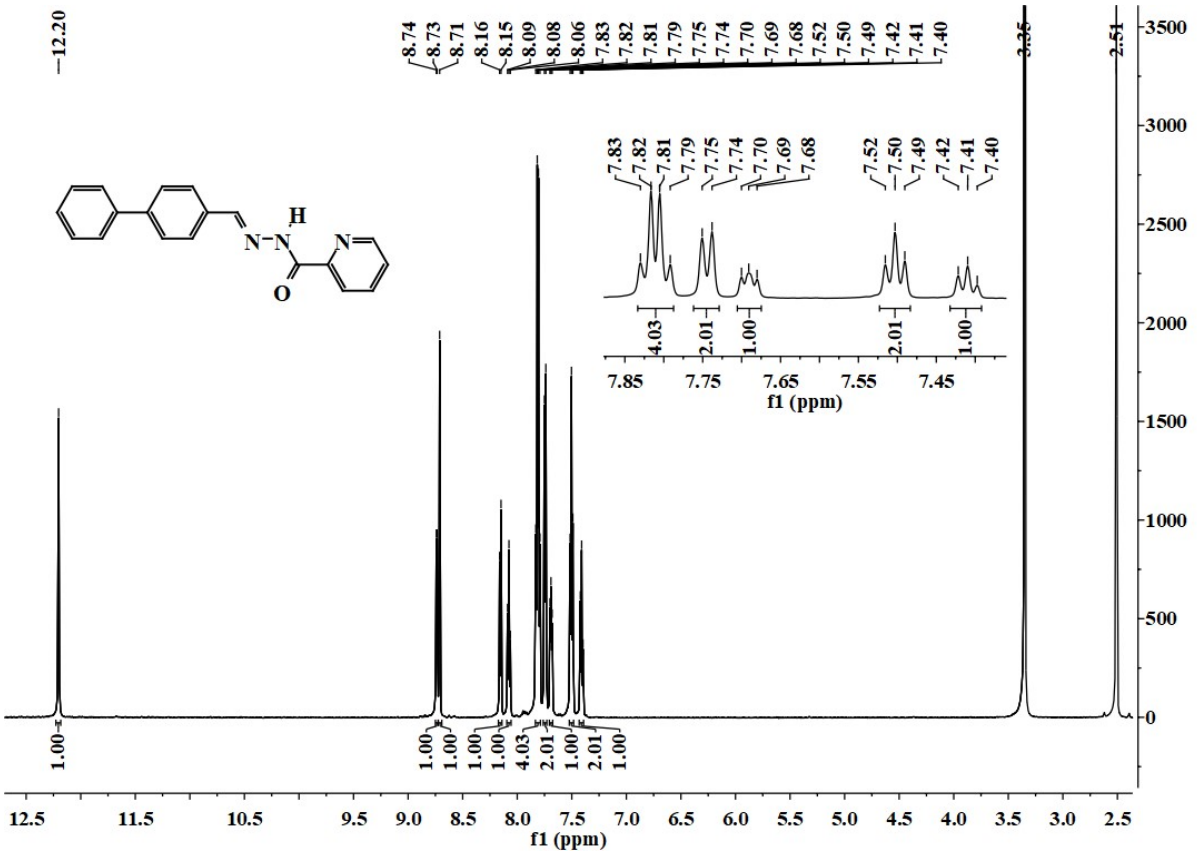

Figure S18. ^{1}H NMR (DMSO-d_6, 600 MHz) spectrum of **BPMP**.

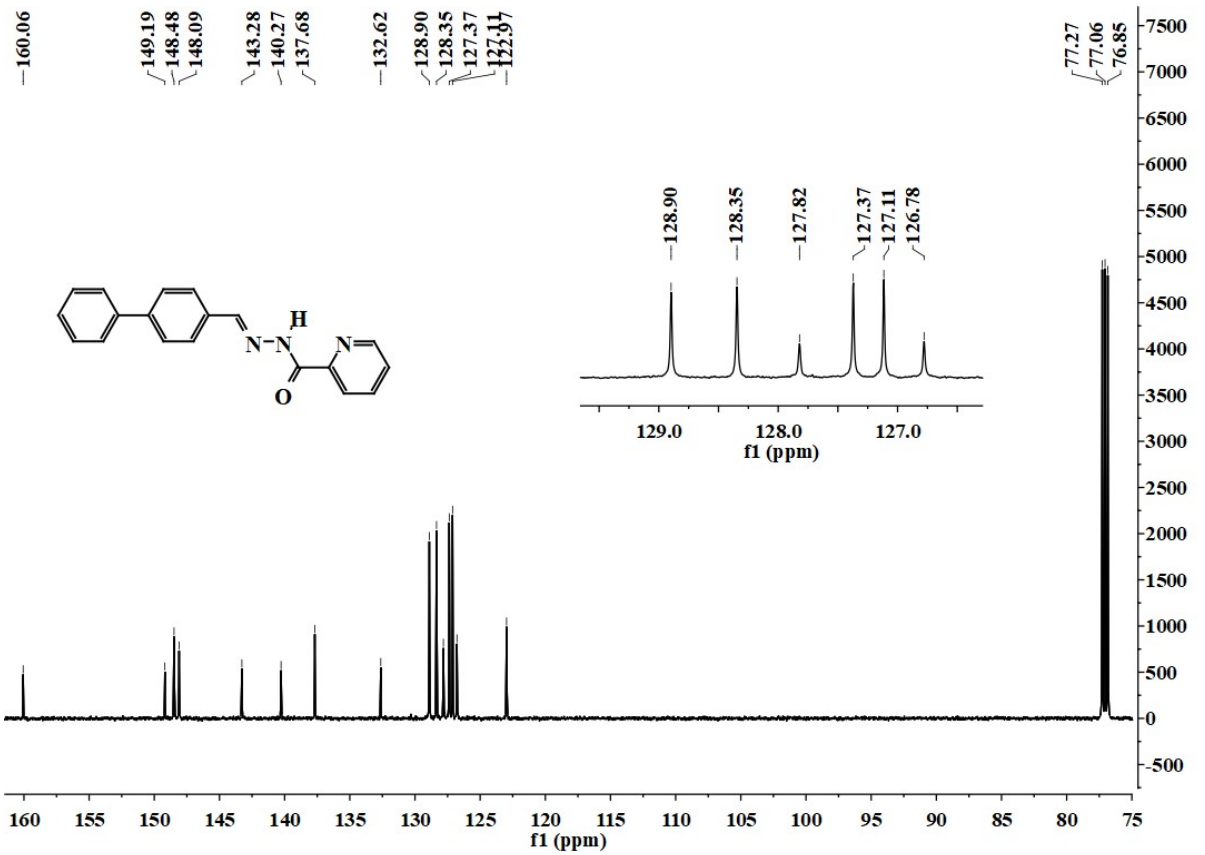

Figure S19. ^{13}C NMR ($CDCl_3$, 151 MHz) spectrum of **BPMP.**

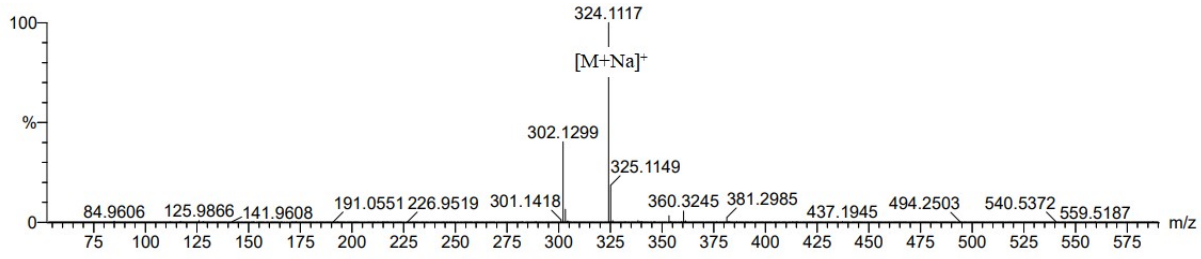

Figure S20. the HR-MS of **BPMP** (in MeOH).

1. A. Miniewicz, H. Orlikowska, A. Sobolewska and S. Bartkiewicz, *Phys. Chem. Chem. Phys*., 2018, **20**, 2904-2913.

2. H. Qian, S. Pramanik and I. Aprahamian, *J. Am. Chem. Soc*., 2017, **139**, 9140−9143.